Cell. Mol. Biol. (ISSN: 1165-158X)

Journal Homepage: www.cellmolbiol.org

Cellular and Molecular Biology

Original Article

Phalaenopsis orchid flower extract attenuates high glucose-induced senescence via Nrf2/HO-1 activation and promotes wound healing in human dermal fibroblasts

Shu-Ling Peng[1#], Chiung-Man Tsai[2#], Chia-Jui Weng[3,*], Shun-Fa Yang[1,4*]

[1] *Institute of Medicine, Chung Shan Medical University, Taichung, Taiwan*
[2] *Chest Hospital, Ministry of Health and Welfare, Tainan, Taiwan*
[3] *Department of Food and Beverage Services, Tainan University of Technology, Tainan, Taiwan*
[4] *Department of Medical Research, Chung Shan Medical University Hospital, Taichung, Taiwan*

Article Info

Article history:

Received: March 25, 2025
Accepted: May 24, 2025
Published: June 30, 2025

Use your device to scan and read the article online

Abstract

Skin aging in diabetic patients is closely associated with delayed wound healing and oxidative stress-mediated fibroblast dysfunction. This study investigated the protective and regenerative effects of a water extract of Phalaenopsis orchid flower (WEPF), an ornamental plant endemic to Taiwan, on high glucose (HG)-induced cellular senescence in human dermal fibroblasts (CCD-966SK), with a focus on the Nrf2/HO-1 antioxidant pathway. Cytotoxicity, cellular senescence, and ROS production were respectively assessed using MTT assay, senescence-associated β-galactosidase (SA-β-gal) staining, and DCFDA-cellular reactive oxygen species assay. Western blotting and ELISA were used to analyze the cellular senescence-related proteins. Fibroblasts treated with WEPF under HG conditions exhibited reduced senescence-associated β-galactosidase (SA-β-gal) activity, lower ROS levels, and attenuated cell cycle arrest. Protein expression profiling revealed suppression of the p53/p21^{Waf1}, and p16^{INK4a}/Rb pathways and decreased matrix metalloproteinase-1 (MMP-1) expression. Mechanistically, WEPF exerted its effects by activating the Nrf2/HO-1 axis and restoring the expression of senescence marker protein-30 (SMP30), thereby promoting fibroblast repair and reducing pro-inflammatory signaling. These findings support the potential of WEPF as a botanical therapeutic agent for diabetic wound healing and age-related skin deterioration.

Keywords: Water extract of Phalaenopsis orchid flower, Inflammation, Hyperglycemia, Wound healing, Anti-aging.

1. Introduction

Population aging is accelerating globally, with those aged 60 and over expected to rise from 11% in 2011 to 22% by 2050 [1]. In Taiwan, aging has contributed to an increase in chronic diseases, now a leading cause of death. Skin aging is a complex biological process influenced by intrinsic and extrinsic factors. As the body's largest organ and first line of defense, the skin is especially vulnerable to age-related changes. These include reduced elasticity, delayed wound healing, and heightened susceptibility to oxidative stress and inflammation. Accumulating evidence suggests that advanced glycation end products (AGEs), matrix metalloproteinases (MMPs), and chronic inflammation are key contributors to skin aging [2].

AGEs form through non-enzymatic reactions between sugars and proteins, known as Maillard reactions, resulting in oxidative modifications that accumulate over time. These modifications disrupt collagen and elastin function in the skin, reducing elasticity, increasing stiffness, and impairing wound healing [3]. Furthermore, AGEs trigger fibroblast apoptosis, exacerbating extracellular matrix (ECM) degradation and accelerating dermal aging [4]. The interaction between AGEs and collagen leads to an increased expression of proteolytic enzymes, such as MMPs, further amplifying the breakdown of skin structural components.

MMPs are zinc-dependent enzymes that regulate ECM remodeling. Their overactivation contributes to skin thinning and wrinkle formation. UVB-induced oxidative stress increases MMP-1, which disrupts collagen homeostasis [5], while MMP-2 and MMP-9 facilitate the final breakdown of type I collagen [6,7]. Chronic inflammation and hyperglycemia further elevate MMP activity, worsening ECM degradation and promoting skin aging.

Wound healing is a multifaceted process involving coordinated actions of cells, cytokines, and ECM components. Aging, diabetes, and chronic inflammation disrupt these interactions, leading to delayed wound closure and persistent tissue damage [8,9]. Senescent cells accumulate at wound sites, releasing pro-inflammatory cytokines that impair normal tissue repair mechanisms [10-12]. In the early phases of wound healing, coagulation and inflam-

* Corresponding author.
E-mail address: t10044@mail.tut.edu.tw (S-F. Yang).
# These authors contributed equally
Doi: http://dx.doi.org/10.14715/cmb/2025.71.6.15

matory responses are triggered to control bleeding and initiate repair. However, in aging skin, the inflammatory phase is prolonged, resulting in excessive oxidative stress and ECM degradation. Key pathways such as mitogen-activated protein kinase (MAPK) and transforming growth factor-beta (TGF-β)/SMAD regulate fibroblast migration and collagen deposition, both essential for healing [12-15]. Dysregulation of these pathways can lead to excessive scarring or impaired wound closure.

Chronic hyperglycemia, a hallmark of diabetes, is a major contributor to oxidative stress and inflammation in aging skin. Elevated glucose levels increase reactive oxygen species (ROS) production via mitochondrial overactivity and polyol pathway activation [16]. ROS accumulation induces oxidative stress, leading to DNA damage, lipid peroxidation, and protein oxidation. Studies have shown that diabetic patients exhibit elevated ROS levels, contributing to endothelial dysfunction and impaired skin repair [17]. Oxidative stress disrupts redox homeostasis, promoting cellular senescence and inflammation. The senescence-associated secretory phenotype (SASP) further exacerbates chronic inflammation by releasing cytokines such as interleukin-6 (IL-6), interleukin-8 (IL-8), and tumor necrosis factor-alpha (TNF-α) [18]. Nrf2 is a key transcription factor that regulates the antioxidant response element (ARE)-mediated expression of detoxifying and antioxidant enzymes, including Heme oxygenase-1 (HO-1). Activation of the Nrf2/HO-1 pathway mitigates oxidative damage, reduces senescence, and supports tissue repair under hyperglycemic conditions [19,20].

Cellular senescence is a defining feature of aging and is characterized by irreversible cell cycle arrest. High glucose levels have been shown to induce premature senescence in dermal fibroblasts by activating SASP-related pathways [21]. The p53/$p21^{Waf1}$ axis plays a crucial role in regulating cell cycle progression and DNA damage responses. In response to oxidative stress, p53 upregulates $p21^{Waf1}$, leading to inhibition of cyclin-dependent kinase (CDK) activity and subsequent cell cycle arrest [22]. The activation of SASP factors further amplifies inflammation, creating a feed-forward loop that sustains cellular aging.

Orchidaceae, comprising around 800 genera and 30,000 species, are valued not only for their ornamental appeal but also for their pharmacological potential. Orchids contain bioactive compounds such as alkaloids, flavonoids, anthocyanins, and steroids-with antioxidant, anti-inflammatory, anticancer, and cardiovascular effects [23]. Rhizome extracts are rich in glycopeptides that enhance fructosamine 3-kinase (FN3K) activity, reduce collagen glycation, and stimulate fibroblast growth factor-beta (FGF-β) and transforming growth factor-beta (TGF-β) secretion, facilitating cellular regeneration and delaying skin aging [24,25]. Despite Orchidaceae's diversity, the bioactivities of *Phalaenopsis* species remain underexplored, especially their water-soluble compounds. Preliminary studies suggest the presence of antioxidant polyphenols and flavonoids in *Phalaenopsis* flower extract [26], highlighting its potential as a novel anti-aging agent.

Hyperglycemia, a hallmark of diabetes, impairs wound healing, accelerates skin aging, and drives chronic inflammation. High glucose (HG) conditions induce excessive ROS, which act as secondary messengers triggering the SASP, leading to DNA damage, cell cycle arrest, and aging. While many anti-aging compounds have been studied, the effects of water extract from Phalaenopsis orchid flowers (WEPF), a specialty of Tainan, remain underexplored. This study examines WEPF's impact on HG-induced senescence in human dermal fibroblasts (CCD-966SK) and its wound-healing potential. By investigating key senescence-related proteins, we aim to clarify whether WEPF modulates the Nrf2/HO-1 signaling pathway to counteract oxidative stress and senescence. These findings may establish Phalaenopsis as a promising botanical agent for treating diabetic skin aging and impaired wound repair.

2. Materials and Methods

2.1. Materials and Reagents

WEPF was supplied by Charm Sun phalaenopsis Biotechnology Co., Ltd. In Tainan. 3-(4,5-dimethylthiazol-2-yl)-2,5-diphenyltetrazoliumbromide (MTT) and DMSO were purchased from Sigma-Aldrich Co. (St. Louis, MO). Modified Eagle's medium (MEM)-875545 medium, fetal bovine serum (BSA), non-essential amino acid (NEAA), and sodium pyruvate were purchased from Invitrogen Co. (Carlsbad, CA). Human IL-6 ELISA Ready-SET-Go kit was purchased from eBioscience (San Diego, CA). Nuclear/Cytosolic Fractionation kit was purchased from BioVision Inc. (Mountain View, CA). Total anti-lamin B1, anti-β-actin, and the total and phosphorylated anti-p53, anti-p21, and anti-p16 antibodies were purchased from Cell Signaling Technology (Beverly, MA). Total anti-Cdk2, anti-pRb, anti-HO-1, anti-Nrf2, anti-SMP-30, and anti-Smad3 were purchased from Millipore Co. (Billerica, MA). Matrigel was purchased from BD Biosciences (San Jose, CA).

2.2. Cell culture

Human dermal fibroblasts (HNDFs, CCD-966SK) were obtained from the Bioresource Collection and Research Center (BCRC, Food Industry Research and Development Institute, Hsin Chu, Taiwan) and grown in MEM medium, which supplemented with 10% (v/v) fetal bovine serum (FBS), 1% PS antibiotic solution (100 units/mL penicillin, 100 μg/mL streptomycin), 0.37% (w/v) $NaHCO_3$, 0.1 mM NEAA, and 1mM sodium pyruvate, at 37 °C in a humidified atmosphere of 95% air and 5% CO_2.

2.3. Cell viability assay

Cell viability was determined by MTT assay. Cells were cultured in MEM medium and seeded onto 24-well plates (1×10^6 cells/well) and incubated for 24 h at 37 °C. Then, the cells were treated with each compound at the indicated concentration and incubated for the indicated time. The dye solution (10 μL; 5 mg of dye/1 mL phosphate-buffered saline, PBS) was added to each well for an additional 1 h of incubation at 37 °C. After the addition of DMSO (100 μl/well), the reaction solution was incubated for 30 min in the dark. The absorbance at 570 and 630 nm (reference) was recorded with a Fluostar Galaxy plate reader (BMG LabTechologies, GmbH, Offenburg, Germany). The percent viability of the treated cells was calculated as follows:

[(A570nm-A630nm)sample/(A570nm-A630nm) control]× 100

2.4. Cell proliferation assay

Cells were cultured in MEM medium and seeded onto 24-well plates (1×10^6 cells/well) and incubated for 24 h at

37 °C. Then, the cells were treated with each compound at the indicated concentration and incubated for further 72 h. Removed the medium and 1000 µL 0.4% w/v trypan blue was added to each well for 10 min of incubation at 37 °C. Observed the ratio of living cells (without dying) to total cells under microscope.

2.5. Cell-cycle analysis

Cells were cultured in MEM medium and seeded onto 10 cm dish (5×10^5 cells/dish) and incubated for 24 h at 37 °C. Then, the cells were treated with each compound at the indicated concentration and incubated for further 72 h. Removed medium and washed twice with PBS. Added 95% ethanol to each dish and kept in -20°C refrigerator overnight. Next day, washed cells with PBS following removed PBS by centrifugation for 5min. Then, 1 mL PI/Triton X-100 (20 µg/mL PI, 0.1% Triton X-100, and 0.2 mg/mL RNAse) to cells and reacted on ice for 30 min. in the dark.

2.6. Preparation of nuclear/cytosolic extracts

The cells with or without compound treatment were centrifuged (800 rpm) at 4°C for 6 min and were lysed using Nuclear/Cytosolic Fractionation kit. Briefly, the cell lysate was centrifuged by 16,000×g at 4°C for 5 min after the additions of CEB-A and CEB-B mix. The supernatant portion was removed to a new Eppendorf as the cytosolic extract, and the precipitation portion was added by 100 µl NEB mix and vortexed for 15 s. After centrifuging by 16,000×g at 4°C for 10 min, the upper soluble portion was collected as nuclear extract.

2.7. Western blotting

Ten micrograms of cytosolic or nuclear extracts were separated by SDS-PAGE on 10% polyacrylamide gel and transferred onto a cellulose nitrate membrane (Sartorius Stedim Biotech GmbH, Goettingen, Germany) using Bio-Rad Mini Protean electrotransfer system. The blot was subsequently blocked with 5% skim milk in PBST for 1 h and probed with primary antibody at 4 °C overnight. Detection was performed with an appropriate horseradish peroxide-conjugated secondary antibody at room temperature for 1 h. The signal intensity was visualized by chemiluminescent ECL detection system (Millipore) and quantified by Biospectrum AC Imaging System (UVP, Upland, CA, USA). The nuclear and cytosolic protein levels were normalized relative to laminB1 and β-actin, respectively.

2.8. Cellular senescence assay

Cellular senescence detection kit (ab65351) was used to quantify the aged cells. Cells were seeded onto 24-well plates at a number of 5×10^5 cells/well in MEM medium. After 24 h of incubation, the cells were treated with the indicated concentration of glucose for 72 h or pretreated with WEPF for 24 h following treated with glucose for 72 h. Removed medium and washed twice with PBS. Added 200 µL 1X Fixative Solution in each well and reacted 5 min. at room temperature. Removed solution and washed three times with PBS. The dye solution (Staining Buffer and 1 mg X-gal /mL) 400 µL was added to each well and incubated overnight at 37°C in the dark. The numbers of SA-β-gal positive cells were calculated triply by cell counter.

2.9. Enzyme-linked immunosorbent assay

Cells were cultured in a 6-well tissue plate and incubated in a serum-free medium with or without compound for 24 h. The conditioned medium was collected to assay the levels of TNF-α and IL-6 secretion following the manufacturer's instructions for each specific ELISA kit.

2.10. Determination of endothelial nitric oxide production

Production of nitric oxide (NO) by cells was measured as nitrite, the NO stable oxidation form, using Nitrate/Nitrite colorimetric assay kit. Briefly, 80 µL of the culture medium was mixed with 10 µL Enzyme Cofactor Mixture and 10 µL Nitrate Reductase Mixture. Following 1 h of dark incubation to convert nitrate to nitrite, 50 µL Griess reagent A (containing sulfanilamide) and 50 µL Griess reagent B [containing N-(1-Naphthyl) ethylenediamine] were added. After reacting for 10 min at room temperature, total nitrite was measured at 550 nm using iMarkTM Microplate Absorbance Reader (BIO-RAD, JAPAN).

2.11. Intracellular ROS production assay

Intracellular ROS generation was detected using a fluorescent probe, 5-(and-6)-carboxy-2',7'-dichlorodihydro-fluoresceindiacetate (DCF-DA, Molecular Probes, Eugene, OR, USA). DCF-DA readily diffuses through the cell membrane and is enzymatically hydrolyzed by intracellular esterase to form non-fluorescent DCFH, which is then rapidly oxidized to form highly fluorescent DCF in the presence of ROS. The DCF fluorescence intensity is parallel to the amount of intracellular ROS. Cells were cultured in MEM medium and seeded onto 24-well plates (4×10^5 cells/well) and incubated for 24 h at 37 °C. Then, the cells were treated with each compound at the indicated concentration and incubated for further 72 h. At the end of incubation, cells were collected and resuspended in PBS. An aliquot of the suspension was loaded into a 24-well plate, and 500 µL of DCF-DA was added (final concentration: 20 µM). The DCF fluorescence intensity was detected at different time intervals using FLUOstar galaxy fluorescence plate reader (BMG Labtechnologies, Offenburg, Germany) with an excitation wavelength at 485 nm and emission wavelength of 530 nm.

2.12. Wound-healing assay

Cells were grown to 90% confluence in a 6-well plate at 37°C, 5% CO_2 incubator. A wound was created by scratching cells with a sterile 200 µl pipette tip, cells were washed twice with PBS to remove floating cells and then added to a medium with various concentrations (25, 100, 200 µg/mL) of compounds. Photos of the wound were taken each 12 h under ×100 magnitude microscope.

2.13. Protein content determination

The protein content was determined according to the method described by Bradford [27] with bovine serum albumin as a standard.

2.14. Statistical analysis

Data are indicated as the mean ± SD for three different determinations. Statistical comparisons were made by means of one-way analysis of variance followed by Duncan's multiple-comparison test. Values of $p < 0.05$ were considered statistically significant.

3. Results

3.1. Effect of glucose and WEPF on the Viability of CCD-966SK Cells.

The viability test of cells was determined by an MTT assay, which is used for measuring the metabolic activity of a cell. The absorbance decrease in this assay could be a consequence of either cell death or the reduction of cell proliferation. CCD-966SK cells were treated with glucose at various concentrations (0, 15, and 30 mM) or with WEPF (200 µg/mL) for 72 h, and the viability of cells was not significantly reduced. The viability of cells was decreased by 8 and 11% after incubation with 15 and 30 mM, respectively, of glucose for 72 h as compared with control (Figure 1A). The cell viability also was not significantly affected by treatment of 200 µg/mL WEPF for 72 h (data not shown).

3.2. High concentration of glucose (HG) induced and WEPF reduced aging of CCD-966SK cells.

A colorimetric method to detect SA-β-Gal landmark, which facilitated identification of the senescent cells in human and rodent cells, is the most widely used tool to detect aged cells in vitro and in vivo [28]. Figure 1B showed that CCD-966SK cells were significantly induced to aging by 30 mM high glucose (HG) treatment for 72 h. Nevertheless, the pretreatment of WEPF at a concentration of 200 µg/mL on cells was able to reduce the HG-induced senescence significantly ($p < 0.01$) (Figure 1C).

3.3. WEPF released the HG-induced growth arrest in CCD-966SK cells.

After cells were incubated in MEM-875545 medium (10% FBS) without glucose (control), with HG (30 mM), and with HG (30 mM)/WEPF (200 µg/mL) for 72 h, the cell cycle distribution was measured by flow cytometer using PI. The results revealed that HG retarded the cell cycle progress and WEPF released it (Figure 2A). Meanwhile, the MTT assay exhibited insignificant differences in cell viability (Figure 2B) and cell proliferation assay showed HG-decreased ($p < 0.05$) and WEPF-increased ($p < 0.05$) proliferative rate significantly (Figure 2C). Both evidences might support the argument of cell cycle distribution.

3.4. Effect of WEPF on HG-induced cell cycle arrest-related protein expression in CCD-966SK cells.

HG environments induce cell cycle arrest, and genes involved in regulating SASP are significantly upregulated, leading to cellular aging and persistent inflammatory responses. This occurs through the activation of the p53/$p21^{Waf1}$ and $p16^{INK4a}$ signaling pathways, which inhibits cell growth and proliferation. When DNA is damaged, the expression of p53 increases, promoting the activation of $p21^{Waf1}$. $p21^{Waf1}$ inhibits cyclin E/CDK2, further preventing the phosphorylation of Rb proteins. Additionally, $p21^{Waf1}$ and $p16^{INK4a}$ inhibit CDK, further blocking DNA

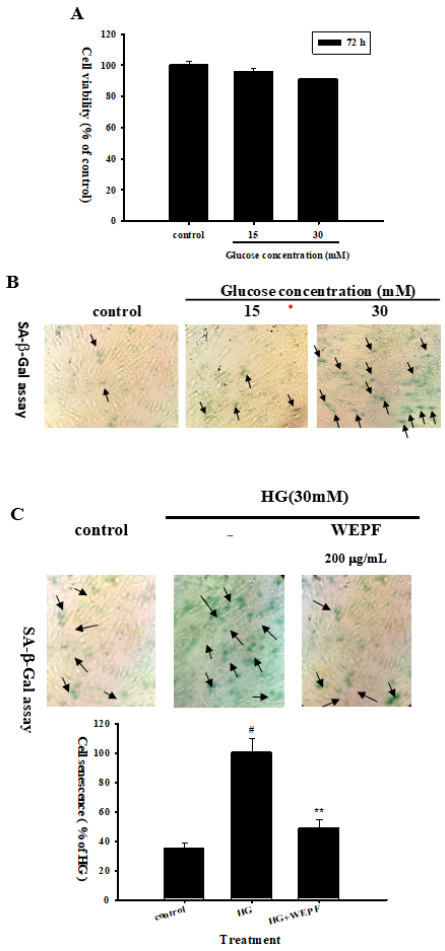

Fig. 1. Determination of glucose concentration for inducing cell aging and WEPF inhibited the HG-induced senescence of cells. CCD-966SK cells were incubated in MEM-875545 medium (10% FBS) without glucose (control), with 15 mM glucose, and with 30 mM glucose (HG) for 72 h. Cell viability was determined by MTT assay with that of control being 100% (A) and cell aging was measured by β-galactosidase assay (SA-β-gal) without (B) or with (C) 200 µg/mL WEPF pre-treatment. Data represent the mean ± SD of three independent experiments. Results were statistically analyzed with Student's t-test. #, indicated $p < 0.05$ compared with the control; **, indicated $p < 0.01$ compared with the HG.

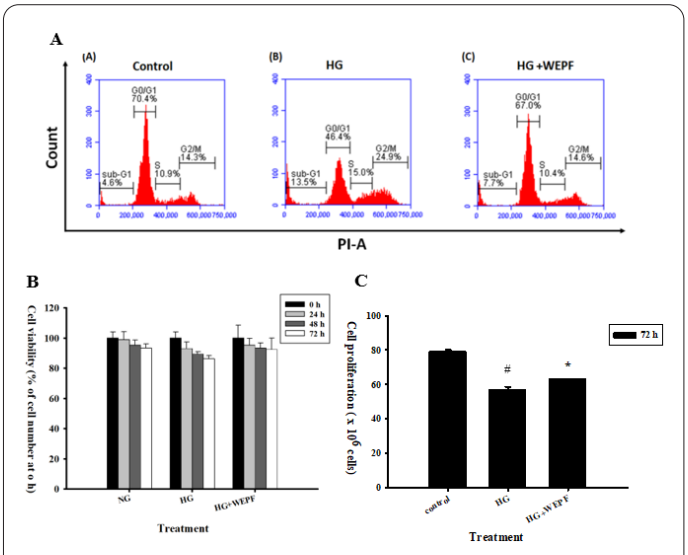

Fig. 2. WEPF released the HG-induced growth arrest in CCD-966SK cells. Cells were incubated in MEM-875545 medium (10% FBS) without glucose (control), with HG (30 mM), and with HG (30 mM)/WEPF (200 µg/mL) for 72 h. Cell cycle distribution was measured by flow cytometer using PI (A). Viability of cells was determined by MTT assay with that of control being 100%. The cell number at 0 h was used as a control (B). Cell proliferation was measured by trypan blue exclusion test (C). Data represent the mean ± SD of three independent experiments. Results were statistically analyzed with Student's t-test. #, indicated $p < 0.05$ compared with the control; *, indicated $p < 0.05$ compared with the HG.

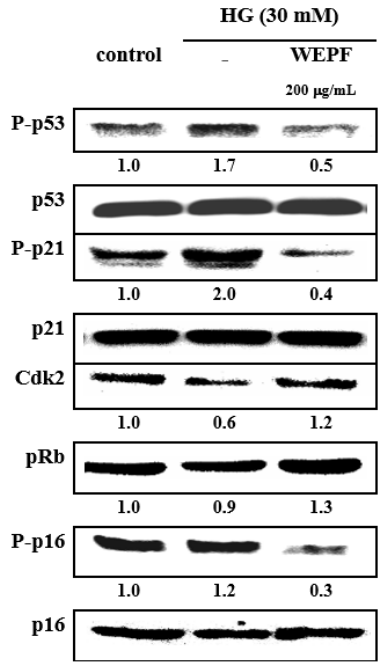

Fig. 3. WEPF released the HG-induced growth arrest of CCD-966SK cells through senescence-associated secretory phenotype (SASP) pathway. Cells were incubated in MEM-875545 medium (10% FBS) with HG (30 mM) only or with WEPF (200 μg/mL), and without glucose as a control. The cell lysates of 24 h incubation was subjected to SDS–PAGE followed by Western blots with anti-p53, anti-p21, anti-p16 (total and phosphorylated for three), anti-Cdk2, and anti-pRb antibodies. Determined activities of these proteins were subsequently quantified by densitometric analyses with that of control being 100%.

replication. As shown in Figure 3, the results demonstrated that HG activates the p53/$p21^{Waf1}$ and $p16^{INK4a}$ signaling pathways resulting in cell cycle arrest. However, the treatment of WEPF on cells released the cell cycle block.

3.5. WEPF negatively modulates HG-induced ROS Production through the promotion of Nrf2-mediated HO-1 Levels in CCD-966SK cells.

WEPF modulated the level of antioxidant enzymes to protect cells against oxidative damage. When using DCF-DA staining to measure the intracellular accumulation of ROS, the ROS formation in cells was accumulated by 30 mM of HG and eliminated by 200 μg/mL of WEPF (Figure 4A). The transcription factor Nrf2 is important in redox homeostasis by regulating the activation of glutathione synthesis and antioxidant defense genes, such as HO-1. We further determined the influence of Nrf2 and HO-1 by HG and WEPF treatment in cells. Levels of HO-1 in cytosolic and Nrf2 in nuclear protein extracts from CCD-966SK cells were distinctly decreased after 30 mM HG incubation and 200 μg/mL WEPF treatment dramatically increased both proteins (Figure 4B). The results indicate that WEPF exhibited an up-regulatory effect on the downstream protein HO-1 and Nrf2 to prevent HG-induced oxidation in CCD-966SK cells.

3.6. WEPF decreased the HG-induced inflammatory factors of CCD-966SK cells.

To investigate the influence of HG and WEPF on the levels of several inflammatory factors (including NO, TNF-α, and IL-6), we treated CCD-966SK cells (10% FBS) without glucose, with HG (30 mM), and with HG (30 mM)/WEPF (200 μg/mL) in MEM-875545 medium for 24 h, and the levels of nitrite, TNF-α, and IL-6 were measured. As a result, the HG-stimulated levels of nitrite, TNF-α, and IL-6 in cells were significantly ($p < 0.05$) sup-

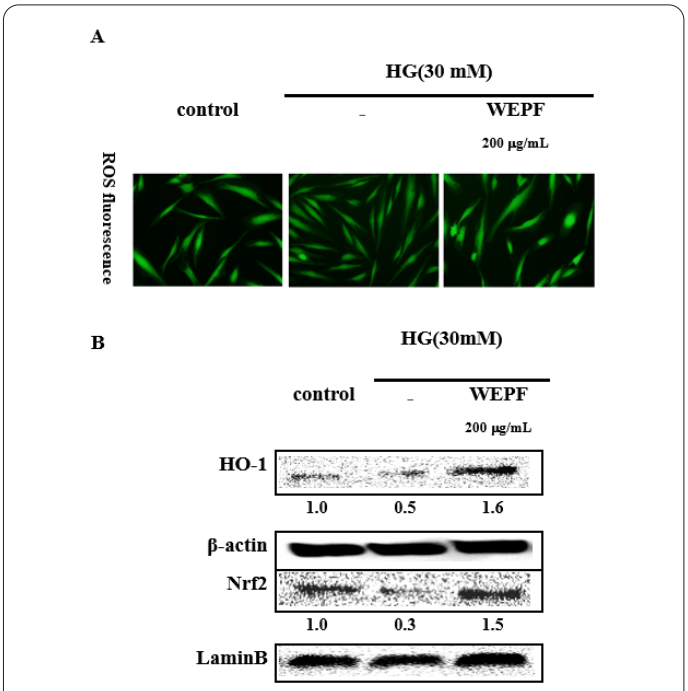

Fig. 4. WEPF decreased the HG-induced oxidative stress of CCD-966SK cells by enhancing HO-1 and Nrf2 levels. Cells were incubated in MEM-875545 medium (10% FBS) without glucose (control), with HG (30 mM), and with HG (30 mM)/WEPF (200 μg/mL). The ROS production was measured by fluorescence detection after treating for 72 h (A). The cell nuclear extracts of 24 h incubation was subjected to SDS–PAGE followed by Western blotting with anti-HO-1 and anti-Nrf2 antibodies. Determined activities of these proteins were subsequently quantified by densitometric analyses with that of control being 100% (B).

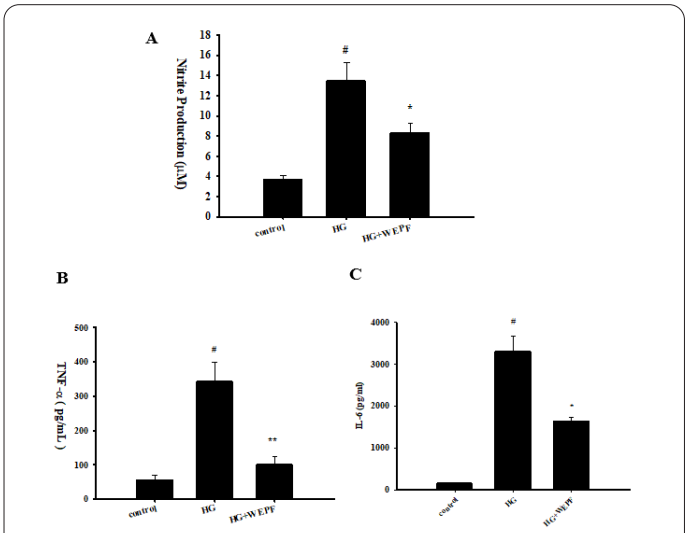

Fig. 5. WEPF decreased the HG-induced inflammation of CCD-966SK cells. Cells were incubated in MEM-875545 medium (10% FBS) without glucose (control), with HG (30 mM), and with HG (30 mM)/WEPF (200 μg/mL) for 24 h. Nitrite (A), TNF-α (B), and IL-6 (C) were detected following the steps describe in Materials and Methods. Data represent the mean ± SD of three independent experiments. Results were statistically analyzed with Student's t-test. #, indicated $p < 0.05$ compared with the control; * and ** indicated $p < 0.05$ and <0.01, individually, compared with the HG.

pressed by the treatment of WEPF (Figure 5). According to the effective concentration, WEPF should be a stronger inhibitor of HG-stimulated intracellular inflammation.

3.7. WEPF up-regulated the HG-depressed SMP30 level in CCD-966SK cells.

SMP30 is a newly known anti-aging factor, which plays a vital role in preventing apoptosis and reducing oxidative stress damage. The level of SMP30 has been found to decline with age and in the HG environment. Our study showed that HG depressed the level of SMP30 in cells, and WEPF recovered it. The data suggested that WEPF exhibited a protective effect against HG-stimulated senescence through up-regulating SMP30 protein (Figure 6).

3.8. Effect of WEPF on type I collagen secretion in CCD-966SK cells.

Collagen is the main component of connective tissue, and TGF-β is a growth factor that promotes collagen secretion by cells. Human dermal fibroblasts are the primary cells responsible for producing collagen and play an essential role in the wound healing process. This study aims to investigate whether WEPF can induce the secretion of collagen in CCD-966SK cells and promote the generation of type I collagen. TGF-β1 was used as the positive control group for comparison. According to the experimental results in Figure 7A, a significant increase in type I collagen was observed as 5 μg/mL TGF-β1 was used to treat cells. Therefore, 5 μg/mL TGF- β1 was used as the concentration for the positive control group in the following experiments. Western blotting was utilized to confirm the secretion of type I collagen in CCD-966SK cells after treatment with different concentrations of WEPF (25-200 μg/mL) for 24 h. The results showed that the secretion of type I collagen protein increases correspondingly as the WEPF concentration increases (Figure 7B).

3.9. Effect of WEPF on the expression of phosphorylated Smad3 protein in CCD-966SK cells.

The main pathway for type I collagen synthesis involves the TGF-β/Smad pathway. According to the results in Figure 7B, the expression of type I collagen increases with the concentration of WEPF. Therefore, we further investigated whether the secretion of type I collagen is mediated through the TGF-β/Smad pathway. Smad3 should be the closest signaling protein related to type I collagen synthesis in this pathway. As the results of the Western blotting experiment shown in Figure 8, it was observed that the phosphorylated Smad3 protein up-expressed as the concentration of WEPF increased. The data might indicate that WEPF up-regulated phosphorylation of Smad3 and leading to a corresponding increase in the expression of type I collagen (compares Figure 7B with Figure 8).

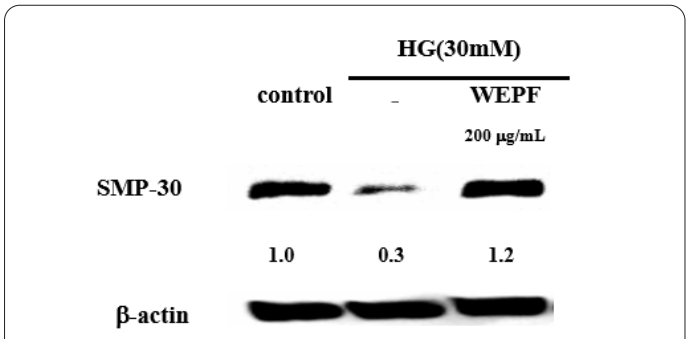

Fig. 6. WEPF enhanced the HG-depressed senescence marker protein (SMP)-30 of CCD-966SK cells. Cells were incubated in MEM-875545 medium (10% FBS) without glucose (control), with HG (30 mM), and with HG (30 mM)/WEPF (200 μg/mL) for 72 h. The cell lysates were subjected to SDS–PAGE followed by Western blots with anti-SMP-30 antibodies. Determined activities of these proteins were subsequently quantified by densitometric analyses with that of control being 100%.

3.10. WEPF inhibits the MMP-1 protein expression and promotes migratory ability of CCD-966SK cells

To clarify whether the MMP-1 protein was involved in the migration of CCD-966SK cells or not, we analyzed the

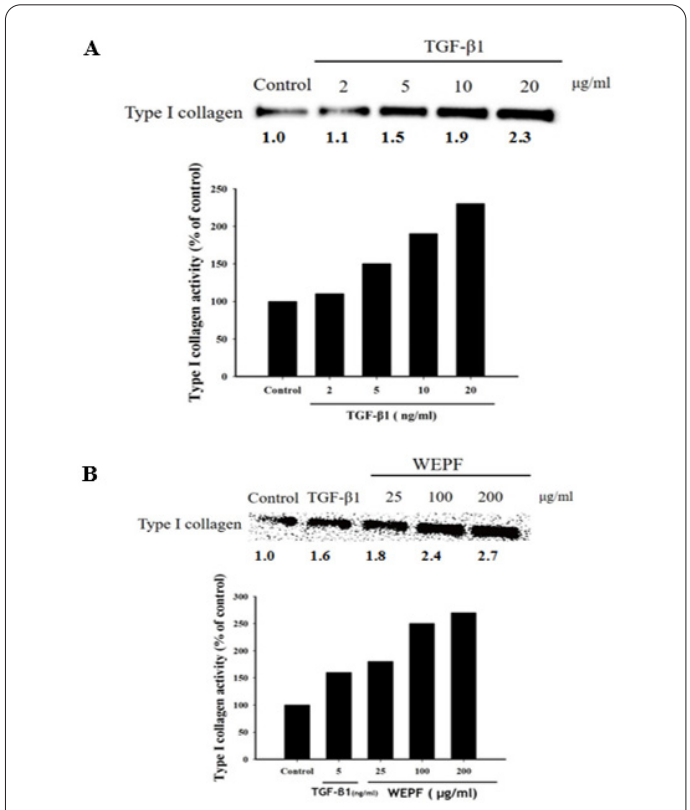

Fig. 7. Determined a concentration of TGF-β1 on type I collagen protein expression, and effect of WEPF on TGF-β1-induced type I collagen protein expression in CCD-966SK cells. Cells were in the presence of various concentrations (2-20 μg/mL) of TGF-β1 for 24 h and detected type I collagen protein (A). Cells were incubated with or without TGF-β1 (5 μg/mL) in the presence of various concentrations (25-200 μg/mL) of WEPF for 24 h and detected type I collagen protein (B). Values are expressed as mean ± S.D. of three replicates.

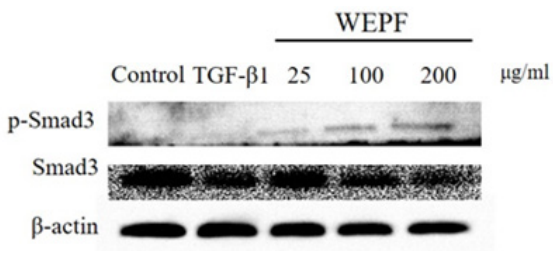

Fig. 8. Effects of WEPF on the activation of Smad3 in CCD-966SK cells. Phosphorylation and total protein expression of Smad3 signaling proteins were analyzed in whole cell lysates using Western blots. Determined activities of these proteins were subsequently quantified by densitometric analyses with that of control being 100%

effects of WEPF on MMP-1 and migration of the cells. The results shown in Figure 9A demonstrated that the level of MMP-1 protein in CCD-966SK cells was decreased correspondingly to the increased WEPF dose. On the contrary, the migratory ability of CCD-966SK cells increased following the 48 treatments of different concentrations (25, 100, 200 μg/mL) of WEPF was observed (Figure 9B). The data suggest that WEPF should be a positive agent to promote wound healing by inhibiting MMP-1 protein expression and enhancing migration of CCD-966SK cells.

4. Discussion

Aging is a complex biological process influenced by environmental, genetic, and epigenetic factors. Chronic inflammation is a hallmark of aging and is linked to increased morbidity and mortality in the elderly [29-30]. Mild, systemic inflammation is associated with age-related diseases, including type 2 diabetes (T2D) and its complications. Low-grade systemic inflammation contributes to T2D and its complications, though underlying mechanisms remain unclear. Emerging evidence implicates cellular senescence and SASP play a crucial role in disease progression. In diabetic patients, hyperglycemia and AGEs trigger oxidative stress and inflammation, leading to impaired wound healing, foot ulcers, and accelerated skin aging [31,32].

Certain bioactive compounds, such as polyphenols, flavonoids, and terpenoids, possess antioxidant properties that reduce inflammation and oxidative stress, thereby slowing cellular aging [33,34]. Orchidaceae extracts, rich in alkaloids, flavonoids, carotenoids, anthocyanins, steroids, and glycopeptides, have shown potential in reversing glycation in fibroblasts [25,35] and may offer therapeutic benefits for diabetes, wound healing, and anti-aging.

This study established a fibroblast model (CCD-966SK) to investigate high glucose-induced senescence. Previous studies have shown that HG (>25 mM) increases oxidative stress and induces premature senescence compared to normal glucose (5.5 mM), confirming the relationship between glucose concentration and stress-induced premature senescence (SIPS) in fibroblast cultures [36]. Targeting inflammatory mediators like iNOS, COX-2, TNF-α, and IL-6 can mitigate ROS-induced damage and delay senescence-related skin deterioration [37]. Our results (Figure 1B) showed that 30 mM glucose-induced cellular aging (consistent with the findings by Zhao et al. [38] who used the same concentration to increase ROS in astrocytes), significantly increasing IL-6 and TNF-α levels at 48 h, followed by SA-β-gal–positive staining at 72 h (Figure 1B).

To evaluate the protective effects of WEPF, fibroblasts were co-cultured with 30 mM HG and 200 μg/mL WEPF. MTT assays confirmed no cytotoxicity at this concentration. WEPF significantly reduced ROS production (Figure 4A) and SA-β-gal activity (Figure 1C), indicating antioxidant potential. Consistent with previous studies [39,40], HG exposure upregulated senescence markers $p16^{INK4a}$, $p21^{Waf1}$, and p53 after 72 h. WEPF treatment suppressed these markers, particularly $p16^{INK4a}$ and $p53/p21^{Waf1}$ (key regulators of cell cycle arrest), suggesting its role in attenuating HG-induced cellular senescence (Figure 3).

Cell cycle arrest is a hallmark of senescence, with senescent cells irreversibly stalled in the G0/G1 phase. Our data showed that HG reduced the G0/G1 population, while

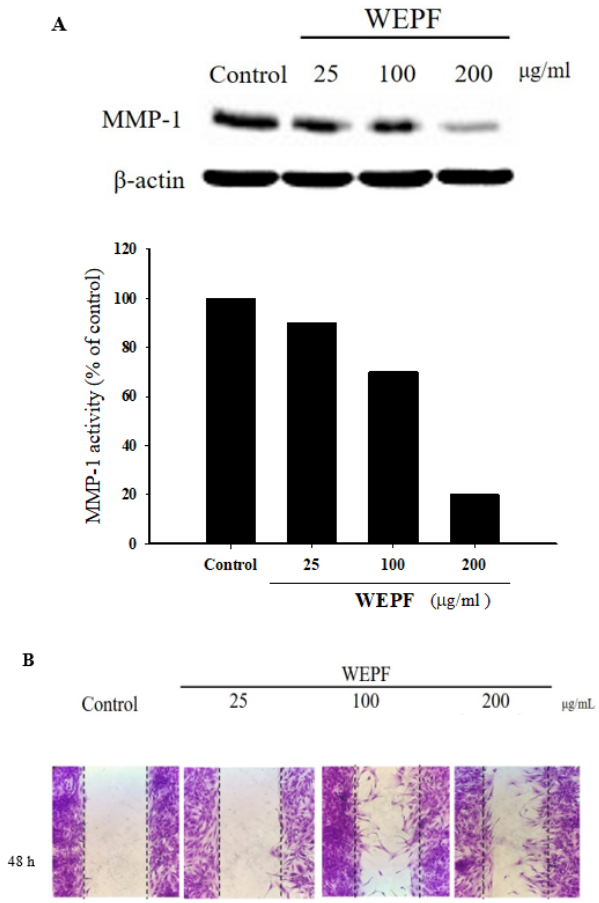

Fig. 9. Effects of WEPF on MMP-1 protein expression and wound healing in CCD-966SK cells. Cells were treated with various concentrations (25-200 μg/ml) of WEPF for 24 h. MMP-1 protein expression was measured by Western blots (A). Cells were treated with or without the indicated concentrations of WEPF in a serum-free media for 48 h and proceeded wound healing test. Photos of the wound were taken under ×100 magnitude microscope (B).

WEPF restored it to control levels (Figure 2A). HG also suppressed CDK2 expression and pRb phosphorylation—key regulators of the G1-S transition [35]—but WEPF reversed these effects, supporting its role in preventing cell cycle arrest (Figure 3).

Eukaryotic cells rely on primary and secondary antioxidant defense mechanisms, particularly phase II detoxification enzymes such as HO-1, NQO1, and GST, which neutralize toxic molecules before they induce DNA damage. Studies indicate that polyphenols, flavonoids, terpenoids, vitamins, and resveratrol protect against oxidative stress and aging [41]. A 2024 study further demonstrated the pivotal role of the Nrf2/HO-1 pathway in accelerating diabetic wound healing [42]. Our study found that WEPF significantly inhibited HG-induced ROS generation (Figure 4A). Western blot analysis confirmed that WEPF upregulated Nrf2, increasing HO-1 expression (Figure 4B), further supporting its antioxidant potential.

Fibroblasts are key to wound healing through proliferation, migration, and ECM production, including collagen. MTT assays confirmed that WEPF (25–200 μg/ml) was non-toxic. While MMP-1 aids in re-epithelialization, excessive levels disrupt granulation tissue formation [43]. Our results (Figure 9A) showed that WEPF inhibited MMP-1, helping preserve type I collagen integrity.

TGF-β1 regulates collagen synthesis by promoting type I and III collagen production and stimulating fibro-

blast proliferation [44–46]. Our study found that WEPF increased type I collagen production in a dose-dependent manner (Figure 7B), supporting its role in wound healing. As Smad3 phosphorylation is key to TGF-β/Smad signaling [47], the observed correlation between WEPF-induced collagen production and p-Smad3 levels (Figure 8) suggests that WEPF promotes collagen synthesis via the TGF-β/Smad pathway to enhance wound healing.

In conclusion, WEPF exhibits antioxidant, anti-inflammatory, and anti-aging properties by reducing ROS, suppressing senescence markers, and enhancing collagen synthesis. These findings suggest that WEPF may serve as a potential therapeutic agent for diabetes-related skin aging and impaired wound healing. Figure 10 provides a visual summary of the biological functions and mechanism of action of WEPF. Further studies are needed to elucidate its molecular mechanisms in vivo.

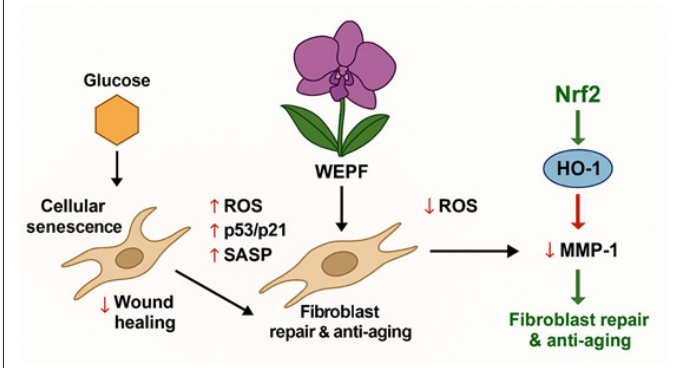

Fig. 10. Schematic illustration of the protective effects of Phalaenopsis orchid flower extract (WEPF) against glucose-induced cellular senescence and its role in promoting wound healing in fibroblasts.

Abbreviations

AGEs, advanced glycation end products; **BSA**, fetal bovine serum; **CDK**, cyclin-dependent kinase; **ECM**, extracellular matrix; **FBS**, fetal bovine serum; **FGF-β**, fibroblast growth factor-beta; **FN3K**, fructosamine 3-kinase; **HNDFs**, human dermal fibroblasts; **HG**, hyperglycemia; **HO-1**, Heme oxygenase-1; **IL-6**, interleukin-6; **IL-8**, interleukin-8; **MAPK**, mitogen-activated protein kinase; **MEM**, modified Eagle's medium; **MMP**, matrix metalloproteinase; **MTT**, 3-(4,5-dimethylthiazol-2-yl)-2,5-diphenyltetrazolium bromide; **NEAA**, non-essential amino acid; **NO**, nitric oxide; **PBS**, phosphate-buffered saline; **ROS**, reactive oxygen species; **SA-β-gal**, senescence-associated β-galactosidase **SASP**, senescence-associated secretory phenotype; **SIPS**, stress-induced premature senescence; **SMP30**, senescence marker protein-30; **TGF-β**, transforming growth factor-beta; **TNF-α**, tumor necrosis factor-alpha; **UVB**, ultraviolet B; **WEPF**, water extract of Phalaenopsis orchid flower.

References

1. United Nations. (2017). World Population Ageing 2017. Department of Economic and Social Affairs, Population Division.
2. Quan T, Wang F, Fisher GJ (2015) Role of age-associated alterations of the dermal extracellular matrix microenvironment in human skin aging: A mini-review. Gerontology 61: 427–435 doi: 10.1159/000371626
3. Ageev AI, Kuznetsov VV (2015) The role of advanced glycation end products in skin aging. Adv Gerontol 5: 303–308 doi: 10.1134/S2079057015040036
4. Farrar MD (2016) Advanced glycation end products in skin ageing and photoageing: What are the implications for epidermal function? Exp Dermatol 25: 947–948 doi: 10.1111/exd.13191
5. Han A, Chien AL, Kang S (2016) Photoaging. Dermatol Clin 34: 291–299 doi: 10.1016/j.det.2016.02.002
6. Aimes RT, Quigley JP (1995) Matrix metalloproteinase-2 is an interstitial collagenase: Inhibitor-free enzyme catalyzes the cleavage of collagen fibrils and soluble native type I collagen generating the specific 3/4- and 1/4-length fragments. J Biol Chem 270: 5872–5876 doi: 10.1074/jbc.270.11.5872
7. Van Doren SR (2015) Matrix metalloproteinase interactions with collagen and elastin. Matrix Biol 44–46: 224–231 doi: 10.1016/j.matbio.2015.01.005
8. Hart J (2002) Inflammation 1: Its role in the healing of acute wounds. J Wound Care 11: 205–209 doi: 10.12968/jowc.2002.11.6.26389
9. Moura LIF, Dias AMA, Carvalho E, de Sousa HC (2013) Recent advances on the development of wound dressings for diabetic foot ulcer treatment—A review. Acta Biomater 9: 7093–7114 doi: 10.1016/j.actbio.2013.03.033
10. Solit DB, Rosen N, Scher HI (2003) Hsp90: A novel target for cancer therapy. J Clin Oncol 21: 4291–4299 doi: 10.1200/JCO.2003.11.023
11. Wang AS, Dreesen O (2018) Biomarkers of cellular senescence and skin aging. Front Genet 9: 247 doi: 10.3389/fgene.2018.00247
12. Wilkinson HN, Hardman MJ (2022) The role of senescent cells in wound healing and ageing. Mech Ageing Dev 204: 111674 doi: 10.1016/j.mad.2022.111674
13. Yue J, Mulder KM (2000) Transforming growth factor-beta signal transduction in epithelial cells. J Cell Biochem 75: 1–9 doi: 10.1002/(SICI)1097-4644(19991001)75:1<1::AID-JCB1>3.0.CO;2-K
14. Kim K, Kim SJ, Kim KH (2004) Transforming growth factor-beta1 induces epithelial to mesenchymal transition of A549 cells. J Biol Chem 279: 40405–40413 doi: 10.1074/jbc.M401364200
15. Massagué J (2012) TGFβ signalling in context. Nat Rev Mol Cell Biol 13: 616–630 doi: 10.1038/nrm3434
16. Bonomini F, Rodella LF, Rezzani R (2015) Metabolic syndrome, aging and involvement of oxidative stress. Aging Dis 6: 109–120 doi: 10.14336/AD.2014.0305
17. Ceriello A (1997) New insights on oxidative stress and diabetic complications may lead to a "causal" antioxidant therapy. Diabetes Care 20: 1830–1836 doi: 10.2337/diacare.20.11.1830
18. Wang AS, Dreesen O, Campisi J (2013) Biomarkers of cellular senescence and skin aging. Front Genet 4: 247 doi: 10.3389/fgene.2013.00247
19. Ma Q (2013) Role of Nrf2 in oxidative stress and toxicity. Annu Rev Pharmacol Toxicol 53: 401–426
20. Loboda A, Damulewicz M, Pyza E, Jozkowicz A, Dulak J (2016) Role of Nrf2/HO-1 system in development, oxidative stress response and diseases: an evolutionarily conserved mechanism. Cell Mol Life Sci 73: 3221–3247
21. Byun HO, Kang DK, Hwang ES, Yoon G (2016) Replicative senescence of human umbilical vein endothelial cells is accompanied by an increase of senescence-associated secretory phenotype. Mech Ageing Dev 156:28–34. https://doi.org/10.1016/j.mad.2016.04.002
22. Kyle S, Werner E, Linden J (2015) The role of p53 in cutaneous squamous cell carcinoma. J Invest Dermatol 135:1712–1715. https://doi.org/10.1038/jid.2015.129
23. Pérez E (2010) Medicinal orchids in the treatment of age-related diseases. Fitoterapia 81:653–661. https://doi.org/10.1016/j.

fitote.2010.04.009
24. Watanabe K, Hashizume K, Chan YS (2007) Glycation-reducing activity of orchid rhizome extracts. Biosci Biotechnol Biochem 71:711–714. https://doi.org/10.1271/bbb.60572
25. Monnier VM (2006) Intervention against the Maillard reaction in aging. Ann N Y Acad Sci 1067:81–90. https://doi.org/10.1196/annals.1354.011
26. Chen YJ, et al. (2019) Antioxidant activity of orchid flowers: Focus on Phalaenopsis species. J Nat Prod Herb Med 3:45–52
27. Bradford MM (1976) A rapid and sensitive method for the quantification of microgram quantities of protein utilizing the principle of protein-dye binding. Anal Biochem 72:248–254. http://dx.doi.org/10.1016/0003-2697(76)90527-3
28. Dimri GP, Lee X, Basile G, Acosta M, Scott G, Roskelley C, Medrano EE, Linskens M, Rubelj I, Pereira-Smith O, Peacocke M, Campisi J (1995) A biomarker that identifies senescent human cells in culture and in aging skin in vivo. Proc Natl Acad Sci USA 92:9363–9367. https://doi.org/10.1073/pnas.92.20.9363
29. Prattichizzo F, De Nigris V, Mancuso E, Spiga R, Mancini A, La Sala L, Antonicelli R, Testa R, Ceriello A (2016) Inflammageing and metaflammation: The yin and yang of type 2 diabetes. Ageing Res Rev 28:33–46. https://doi.org/10.1016/j.arr.2016.05.003
30. Baechle D, Flanagan K (2023) Chronic inflammation and aging: A pivotal interconnection. Mol Biol Rep 50:2157–2170. https://doi.org/10.1007/s11033-023-08195-2
31. Kochet OV, Popova OV, Borisova TY (2017) Advanced glycation end-products and oxidative stress in diabetic complications. Biochem (Mosc) Suppl B Biomed Chem 11:138–144. https://doi.org/10.1134/S199075081702007X
32. Shen CY, Lu CH, Cheng CF, Li KJ, Kuo YM, Wu CH, Liu CH, Hsieh SC, Tsai CY, Yu CL (2024) Advanced glycation end-products acting as immunomodulators for chronic inflammation, inflammaging and carcinogenesis in patients with diabetes and immune-related diseases. Biomedicines 12:1699. https://doi.org/10.3390/biomedicines12081699
33. Salimifar M, Fatehi-Hassanabad Z, Fatehi M (2013) A review on natural products for controlling type 2 diabetes with an emphasis on their mechanisms of action. Curr Diabetes Rev 9:402–411. https://doi.org/10.2174/15733998113096660044
34. Intharuksa A, Kuljarusnont S, Sasaki Y, Tungmunnithum D (2024) Flavonoids and other polyphenols: Bioactive molecules from traditional medicine recipes/medicinal plants and their potential for phytopharmaceutical and medical application. Molecules 29:5760. https://doi.org/10.3390/molecules29235760
35. Zhang Y, Wang Y, Wang X (2023) Flavonoids and glycopeptides in orchid rhizomes reduce collagen glycation and oxidative stress in human dermal fibroblasts. Antioxidants 12:1201. https://doi.org/10.3390/antiox12061201
36. Yang Y, Song M, Zhu X (2013) High glucose induces premature senescence via upregulation of p53/p21 and downregulation of SIRT1 in human diploid fibroblasts. Cell Biochem Biophys 65:59–66. https://doi.org/10.1007/s12013-012-9412-6
37. Liu HM, Cheng MY, Xun MH, Zhao ZW, Zhang Y, Tang W, Cheng J, Ni J, Wang W (2023) Possible mechanisms of oxidative stress-induced skin cellular senescence, inflammation, and cancer and the therapeutic potential of plant polyphenols. Int J Mol Sci 24:3755
38. Zhao R, Wang Y, Huang Y, Wu H, Jin J, Dong S (2018) High glucose-induced oxidative stress promotes autophagy and apoptosis in mouse astrocytes. Front Endocrinol 9:702. https://doi.org/10.3389/fendo.2018.00702
39. Arumugam T, Ramachandran V, Gomez SB, Schmidt AM, Logsdon CD (2014) S100P-derived RAGE antagonistic peptide reduces tumor growth and metastasis. Clin Cancer Res 20:4942–4954. https://doi.org/10.1158/1078-0432.CCR-13-3344
40. Zheng L, Li M (2023) High glucose promotes and aggravates the senescence and dysfunction of vascular endothelial cells in women with hyperglycemia in pregnancy. J Clin Med 12:1100. https://doi.org/10.3390/jcm12031100
41. Sahin K, Orhan C, Akdemir F, Tuzcu M, Iben C, Sahin N (2020) Anti-aging mechanisms of curcumin and its preventive effects on age-related diseases. Mech Ageing Dev 189:111261. https://doi.org/10.1016/j.mad.2020.111261
42. Kim J, Go MY, Jeon CY, Shin JU, Kim M, Lim HW, Shin DW (2024) Pinitol improves diabetic foot ulcers in streptozotocin-induced diabetes rats through upregulation of Nrf2/HO-1 signaling. Antioxidants (Basel) 26:14(1):15. doi: 10.3390/antiox14010015.
43. Rohani MG, Parks WC (2015) Matrix remodeling by MMPs during wound repair. Matrix Biol 44–46:113–121. https://doi.org/10.1016/j.matbio.2015.03.002
44. Hinz B (2016) Myofibroblasts. Wiley Interdiscip Rev Dev Biol 5:233–255. https://doi.org/10.1002/wdev.218
45. Chen W, Tang Z, Sun Y, Zhang Y, Wang X (2020) Proteomic landscape of TGF-β1-induced fibrogenesis in renal fibroblasts. Sci Rep 10:18558. https://doi.org/10.1038/s41598-020-75989-4
46. Wu CS, Wu PH, Fang AH, Lan CC (2012) FK506 inhibits the enhancing effects of transforming growth factor (TGF)-β1 on collagen expression and TGF-β/Smad signalling in keloid fibroblasts: implication for new therapeutic approach. Br J Dermatol 167:532–541. https://doi.org/10.1111/j.1365-2133.2012.11023.
47. Kim S, Leong A, Kim M, Yang HW (2022) CDK4/6 initiates Rb inactivation and CDK2 activity coordinates cell-cycle commitment and G1/S transition. Sci Rep 12:16810. https://doi.org/10.1038/s41598-022-20769-5